J Mater Sci (2010) 45:2090–2098
DOI 10.1007/s10853-009-3907-8

HTC2009

Wettability of SiC and alumina particles by liquid Bi under liquid Al

I. Budai · G. Kaptay

Received: 31 May 2009 / Accepted: 17 September 2009 / Published online: 30 September 2009

Abstract In this paper a new experimental method to measure contact angle of liquid metals on solid particles under an immiscible second liquid metal is described. This includes efficient mixing of the three-phase system (two immiscible liquid metals with solid dispersed particles) with subsequent solidification. The micrographs of the cross sections of samples are analyzed for the distribution of the particles between the bulk of the two metals and the interface between them. As an alternative, exact positions of the particles can be measured at the interface between the two solidified metals. These two measurements are used to estimate the contact angle of one liquid metal on the solid particles under another, immiscible liquid metal. As an example, contact angle of a liquid Bi-rich alloy on SiC and alumina particles is measured under liquid Al-rich alloy. The liquid Bi-rich alloy was found to wet perfectly (with zero contact angle) alumina particles under liquid Al-rich alloy, while the contact angle on SiC is found to be around 88°. These contact angle data are shown to be relevant to control the stability of liquid metallic emulsions formed between the two immiscible liquid metals stabilized by the solid particles.

I. Budai · G. Kaptay (✉)
Department of Nano-Composites, BAY-NANO Research Institute for Nanotechnology, Egyetemvaros, E/7, 606, 3515 Miskolc, Hungary
e-mail: kaptay@hotmail.com

I. Budai
Faculty of Engineering, University of Debrecen, Otemeto ut 2-4, Debrecen, Hungary
e-mail: budai.istvan@mfk.unideb.hu

G. Kaptay
Department of Nanotechnology, University of Miskolc, Egyetemvaros, E/7, 606, 3515 Miskolc, Hungary

Introduction

Wettability of solid substrates by liquid metals has a high relevance for different technologies and has a long history of both theoretical and experimental study [1, 2]. However, the majority of measurements so far have been performed under vacuum, or at least in the gaseous/vapor phase (see reviews [1, 2] and recent papers in this journal [3–8]), with exceptional measurements performed under fluxes [9].

Very few papers have been found by us with reported contact angle data of liquid metals on solid substrates in the environment of another liquid metal. The first paper on the subject is probably that of Good et al. [10], who measured the borosilicate glass/Hg/Ga system by a differential capillary rise method. In later works, the immersion/emersion technique was used in different modifications [11, 12]. In all these methods (capillary rise and immersion/emersion technique), the product of the interfacial energy and the cosine of the contact angle is the primary measurable quantity. Thus, special additional analysis and observations are needed to divide this complex quantity into the interfacial energy and the contact angle [11–13]. Experimental observations of previous works are collected in Table 1.

In this paper a new method will be developed to determine the contact angle being independent of the liquid/liquid interfacial energy. The method will be validated for the alumina/Bi/Al system measured previously (see Table 1). New data will be reported for the SiC/Bi/Al system. In addition to scientific curiosity, such values have technological relevance in stabilizing immiscible (monotectic) alloys by solid particles [16]. It should be mentioned that in absence of stabilizing solid particles of desired wettability these systems are highly unstable due to gravity and Marangoni convection [17–21]. According to the theory of solid particles stabilized emulsions [22, 23], the

Table 1 Experimental values of contact angles of liquid metals β on solid substrates γ in the environment of liquid metals α (for definition see Fig. 1)

α	β	γ	T (°C)	$\Theta_{\gamma/\beta/\alpha}$ (°)	Source
Ga	Hg	Borosilicate glass	25	0	[10]
Ga	Pb	W	328	20–30	[11]
Ga	Hg	SiO_2	>320	0	[12]
Al	Pb	Al_2O_3	>660	0	[14, 15]
Al	In	Al_2O_3	>660	0	[14, 15]
Al	Bi	Al_2O_3	>660	0	[15]
Al–Cu	Bi–Al	Al_2O_3	<680	>0	[15]
			>680	0	[15]
			700	0	This paper
Al–Si	Bi	SiC	700	88 ± 4	This paper

stability of this new type of materials is expected to depend mostly on the contact angle in the system.

Definitions and theoretical possibilities

Let us consider a binary A–B system with a miscibility gap. According to general thermodynamics, at any temperature above 0 K the pure metals A and B will at least partly dissolve each other. Thus, one should consider phases α and β, both consisting of the same components A and B in different proportions: the A-rich phase is called α, while the B-rich phase is called β. Our treatment, however, is not limited to two-component systems. Both phases α and β can have any number of components. Let us consider the case when equilibrium is achieved in the system, i.e. the partial Gibbs energies of each component equals in the two phases (for this type of studies see [24–31]).

Now, let us bring this two-phase liquid/liquid system into contact with a solid phase, called γ. Let us arrange the phases such that the liquid α phase fully envelopes both the liquid β phase and the solid γ phase. Moreover, let liquid β and solid γ phases to be in contact under the liquid α phase (see Fig. 1). Let us suppose that the volume of the vapor phase surrounding the liquid α phase is relatively small and the system is closed and isothermal. Then, for simplicity, the four-phase equilibrium (vapor/α/β/γ) can be restricted to a three-phase equilibrium (α/β/γ). Now, let us suppose that this three-phase system is in chemical equilibrium, i.e. all phases consist the same components in different equilibrium concentrations. In this paper the following notation will be used:

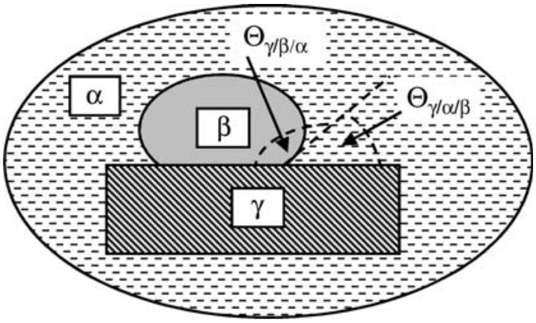

Fig. 1 Definition of the contact angles (see Eq. 1)

- phase α: an Al-rich liquid phase,
- phase β: a Bi-rich liquid phase, and
- phase γ: a SiC-rich or an Al_2O_3-rich solid phase.

The initial composition of the system will uniquely determine the equilibrium mole ratios and compositions of the three phases at given pressure and temperature. These values can be approximately calculated by the Calphad method, or can be measured by the means of analytical chemistry of the equilibrated and quenched samples. Although there will be always some measured and/or calculated uncertainty on the relative amounts and compositions of the equilibrium phases, the initial mole ratio of different components will nevertheless uniquely determine all equilibrium properties of the system at given temperature and pressure. One of those equilibrium properties is the contact angle of liquid phase β on solid phase γ in the environment of liquid phase α, denoted as $\Theta_{\gamma/\beta/\alpha}$. In principle, the contact angle of liquid α on solid phase γ in the environment of liquid phase β can also be defined and noted as $\Theta_{\gamma/\alpha/\beta}$. As follows from Fig. 1, the following relationship exists between these two contact angles:

$$\Theta_{\gamma/\beta/\alpha} + \Theta_{\gamma/\alpha/\beta} = 180^\circ \tag{1}$$

Equation 1 can also be shown to follow from the Young equations written for the two contact angles (not shown here as being straightforward). As Eq. 1 is always valid, only one of the two possible contact angles is an independent thermodynamic quantity. In this paper $\Theta_{\gamma/\beta/\alpha}$ will be chosen as such. If needed, $\Theta_{\gamma/\alpha/\beta}$ can be calculated from Eq. 1. According to the Young equation [32], the contact angle defined in Fig. 1 can be written as:

$$\cos\Theta_{\gamma/\beta/\alpha} = \frac{\sigma_{\gamma/\alpha} - \sigma_{\gamma/\beta}}{\sigma_{\beta/\alpha}} \tag{2}$$

with $\sigma_{i/j}$ being the interfacial energies of the i/j interface, with $i, j = \alpha, \beta$ or γ. Using the Young equation for the droplet of α in vapor environment on solid of γ and the same for droplet β, Eq. 2 can be re-written as:

$$\cos\Theta_{\gamma/\beta/\alpha} = \frac{\sigma_{\beta/v}\cdot\cos\Theta_{\gamma/\beta/v} - \sigma_{\alpha/v}\cdot\cos\Theta_{\gamma/\alpha/v}}{\sigma_{\beta/\alpha}} \tag{3}$$

with $\sigma_{\beta/\mathrm{v}}$ and $\sigma_{\alpha/\mathrm{v}}$ the surface tensions of liquid phases β and α, respectively, while $\Theta_{\gamma/\beta/\mathrm{v}}$ and $\Theta_{\gamma/\alpha/\mathrm{v}}$ are the contact angles of liquids β and α, respectively, on solid γ in the vapor environment. This equation is only valid at coexistence when the chemical potentials of components A and B in α and β phases are identical. Under these circumstances, our requested quantity $\Theta_{\gamma/\beta/\alpha}$ can be calculated from Eq. 3 and from an existing databank of surface tensions of liquid alloys and contact angles of liquid alloys on solid substrates in vapor environment, in combination with a smaller, but still existent databank on liquid/liquid interfacial energies. Unfortunately, the liquid/liquid interfacial energies in liquid metallic systems are lower than the surface tensions in liquid metallic systems by about one order of magnitude [2, 31, 33, 34], what makes the results calculated by Eq. 3 highly uncertain. Moreover, the requested values for Eq. 3 being valid for the exact equilibrium compositions of different phases are practically not available. That is why the contact angle of liquid β on solid γ in the environment of liquid α can be calculated from Eq. 3 only in principle. In practice such calculations are almost impossible today.

Let us demonstrate this situation using a simplified calculation, not taking into account the mutual solubility of liquid Al and Bi and treating Al_2O_3 as an insoluble solid phase in both liquid Al and liquid Bi. At 700 °C the surface tension of pure liquid Al and Bi are about 880 and 350 mJ/m^2 [35], respectively, while the liquid/liquid interfacial energy is only about 50 mJ/m^2 [33, 34, 36, 37]. The contact angle of liquid Al on Al_2O_3 is around 90° [38–42] while liquid Bi does not wet Al_2O_3 with a contact angle of about 149° [40]. Taking these values into account, from Eq. 3 the following value can be calculated for the Al_2O_3/Bi/Al case: $\cos\Theta_{Al_2O_3/Bi/Al} < -5$, i.e. $\Theta_{Al_2O_3/Bi/Al} = 180°$. However, as follows from Table 1, the measured value is rather 0°. This qualitative contradiction can be explained by the simplifications allowed in this calculation. This example is shown here to demonstrate the danger to use Eq. 3 when the conditions of its usage are not met (i.e. when the chemical potentials of components A and B in the α and β phases are not identical).

The above example tells us that first experimental methods should be developed to measure the contact angle $\Theta_{\gamma/\beta/\alpha}$ in immiscible metallic systems. Then, a reliable and as wide as possible databank should be collected before this quantity can be theoretically calculated by any success. The goal of this paper is to make a modest step into this direction.

Experimental procedure

Our goal is to measure the contact angle of a liquid metal on a small solid particle in the environment of another solid metal. This problem is especially relevant to prepare particles stabilized liquid metallic emulsions. In principle, one can prepare large flat samples from small particles. However, this is not always straightforward and practical. Moreover, the surface states of small particles and a large flat sample are not necessarily identical. Therefore, in this paper, a method is developed to estimate the contact angle on small solid particles.

In room temperature colloid science, the position of particles at the interface between two immiscible liquids (usually water and oil phases) is used to measure the contact angle [43–47]. This method is not directly applicable for high-temperature, non-transparent liquid metallic systems. In this paper, a modification to this method is developed. For this, first equilibrium positions of particles should be achieved at high temperature. Then, the positions of the particles should be found from the cross section of the solidified samples. Finally, the requested contact angle should be estimated from the positions of particles in the sample. The experimental procedure developed here is aimed to achieve this goal. In particular, as large as possible interfacial area between liquid phases α and β should be created. For this, dispersive mixing was applied ensuring that the solid particles can freely choose the position they mostly prefer. This can be done using a high-temperature mixer, which allows dispersion of phase β in phase α (or vice versa) and does not allow the sedimentation of particles γ. At the same time, mixing ensures that the physico-chemical equilibrium is achieved in the three-phase system.

The details of the experimental apparatus have been described in details previously [16]. All materials of the apparatus in contact with liquids were made of steel H9, coated by an oxide slurry during experiments to decrease its corrosion and wear. A computer programmable furnace was used with maximum temperature of 1200 °C and heating rate from 1 to 1000 °C/h with accuracy of temperature control of ±5.0 °C. Mixing was performed by a laboratory mixer type MLW MR 25 with a rotational speed between 30 and 2500 min^{-1}.

A model-crucible and mixer were also made of glass with identical geometries as the high-temperature equipment. In this model equipment, the effect of rotational speed was studied on the formation of the emulsion and particle sedimentation using distilled water and 23 vol.% of mercury at room temperature. In this way, the behavior of phases with large density difference such as between Al and Bi was simulated. The optimum value of rotational speed was found around 1000 min^{-1}, ensuring the formation of homogeneous water/mercury emulsion without mixing air into the emulsion. When the rotational speed was much below 1000 min^{-1}, only water is mixed above and around the mercury phase, without the formation of an emulsion. When the rotational speed was much above 1000 min^{-1}, air was mixed into the emulsion. Additional model experiments were performed with a water suspension containing

Table 2 The compositions of the MMCs, the masses of the MMCs and Bi and the initial molar compositions of the studied samples

Sample	MMC	m_{MMC} (g)	m_{Bi} (g)	Initial composition (mol%)
1	Al + 5 vol.% Al_2O_3	97.30	29.85	95.10 Al + 4.01 Bi + 0.89 O
2	(Al + 7 wt% Si + 0.3 wt% Mg) + 20 vol.% SiC	80.40	104.40	65.10 Al + 15.40 Bi + 14.91 Si + 4.36 C + 0.23 Mg

10 vol.% of 45 μm alumina particles. The same rotational speed of 1000 $\min^{-1}$ was sufficient to keep the relatively large alumina particles in homogeneous suspension in water. Thus, the rotational speed of 1000 $\min^{-1}$ was selected to ensure homogeneous distribution of the three phases.

To achieve our goal, three phases (liquid α, liquid β and solid γ) should be mixed avoiding any inner oxidation or formation of bubble inclusions. It is known that the transfer of solid particles from gas into liquid metals is problematic due to high surface tension [48, 49] and the presence of the oxide layer on liquid Al [50]. To avoid this problem, metal matrix composite (MMC) materials with Al-rich matrix reinforced by solid particles (γ = SiC or Al_2O_3) were purchased and used as starting materials in our experiments. In this way, our technology was simplified to mix pure Bi into the Al-matrix MMCs. The types of MMCs, the initial masses and the initial compositions of the two samples are shown in Table 2. The average diameter of particles was 10 μm in all samples.

The weighed specimens of one of the Al-matrix composites and Bi were placed into the crucible. The crucible was kept open, but the constant flow of argon gas with the flow rate of 1 L/min was blown on the surface of the metal to prevent severe oxidation. The crucible was heated with the heating rate of 350 °C/h till the final temperature of 700 °C. The system was kept at this temperature during 1 h for homogenization and equilibration. Then, the mixer was introduced and the system was first mixed with the rotational speed of 50 $\min^{-1}$ during 20 min for further homogenization. After that the emulsification took place with the rotational speed of 1000 $\min^{-1}$ during 5 min. After this emulsification period the mixer was switched off and taken out of the crucible. The crucible was taken out of the furnace and was spontaneously cooled in air.

Once at room temperature, the ingot was sectioned and polished. Scanning electron microscopes (Hitachi S-4800, with Bruker EDX and Hitachi TM-1000 Tabletop Microscope) were used to prepare micrographs and measure the approximate compositions of phases. The position and distribution of particles were measured from the same micrographs as described in the following chapter. The positions of about 100 particles were involved to obtain reliable values for the contact angle in each sample. Experiments with each sample (see Table 2) were repeated twice and more than 10 micrographs after each experiment were prepared to obtain reliable contact angle values.

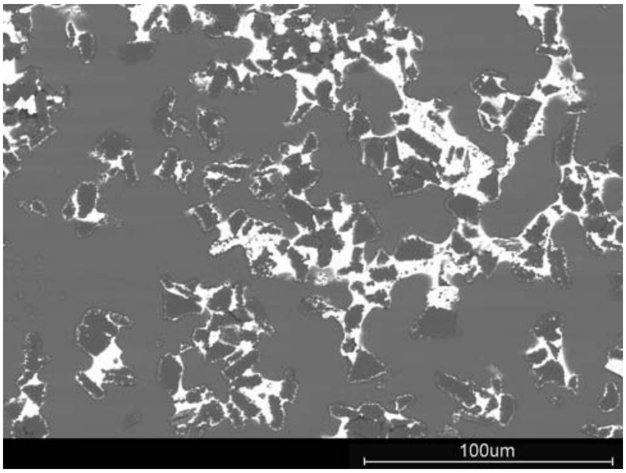

Fig. 2 A typical SEM picture of the cross section of sample 1 (*grey matrix* the Al-rich solidified α phase; *white* the Bi-rich solidified β-phase; *black* Al_2O_3 γ-phase)

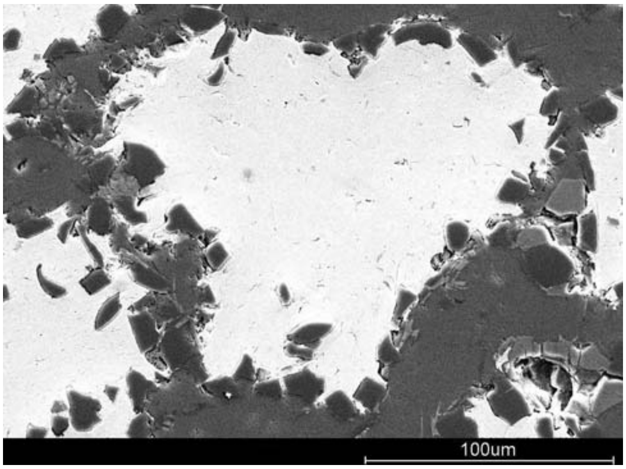

Fig. 3 A typical SEM picture of the cross section of sample 2 (*grey matrix* the Al-rich solidified α phase; *white* the Bi-rich solidified β-phase; *black* SiC-rich γ-phase)

Primary experimental results

Typical SEM pictures of cross sections of the two samples are shown in Figs. 2 and 3. The approximated average compositions of the three phases are given in Table 3. One can see that the compositions agree well with our expectations:

i. Phase α is an Al-rich phase with some dissolved Bi in all cases and some dissolved Si + Mg for sample 2.

Table 3 The approximated equilibrium compositions of phases measured by EDAX (mol%)

Sample	α phase	β phase	γ phase
1	Al + (1.2 ± 0.4) Bi	Bi + (3.4 ± 0.1) Al	(64 ± 7) O + (39 ± 3) Al
2	Al + (7 ± 2) Si + (1.3 ± 0.5) Bi + (0.3 ± 0.1) Mg	Bi + (3.8 ± 0.1) Al + (1.1 ± 0.3) Mg + (0.4 ± 0.1) Si	(53 ± 6) C + (47 ± 4) Si

ii. Phase β is a Bi-rich phase with some dissolved Al in all cases and some dissolved Si + Mg for sample 2.

iii. Phase γ is Al_2O_3 for sample 1 and SiC for sample 2. Studying the distribution of the γ-phase particles, the following preliminary conclusions can be made from Figs. 2 and 3:

   (a) Practically all Al_2O_3 particles are positioned within the Bi-rich β-phase (see Fig. 2),

   (b) The majority of SiC particles are positioned at the interface between the Bi-rich β phase and the Al-rich α phase, with a smaller number of SiC particles within both the Bi-rich β phase and the Al-rich α phase (see Fig. 3).

Evaluation of contact angle

The basic theoretical equation behind our method describes the equilibrium depth of immersion of a spherical particle of radius R into a liquid phase β in the environment of a liquid α [48, 51]:

$$\frac{h_\beta}{R_\gamma} = 1 + \cos \Theta_{\gamma/\beta/\alpha} \tag{4}$$

where h_β is the depth of immersion of particle γ into a liquid phase β. Equation 4 was derived neglecting the role of gravity, thus it is valid only for $R_\gamma < 100$ μm. Equation 4 is visually illustrated in Table 4. The nice feature of Eq. 4 is that it allows to determine the contact angle independently of the liquid/liquid interfacial energy in the system. Let us remind that all the previous methods are most suited to determine the product of the interfacial energy and the cosine of the contact angle (see "Introduction").

Two methods are derived in this paper, being suitable for different situations. Both methods presume that the $\alpha/\beta/\gamma$ system has reached equilibrium and then it was solidified without changing the equilibrium position of γ particles. Then, SEM micrographs are prepared from the cross section of solidified specimen. The solidified α and β phases and the solid γ particles should be distinguishable on these micrographs.

The method based on the position of single particles

Let us suppose that we have good quality micrographs of the cross section of solidified samples, showing at least one solid particle γ at the interface of solidified ex-liquid phases α/β (see Fig. 4). Let us also suppose that the particles are not far from a spherical shape and their position at the α/β interface has not changed during cooling and solidification. Then, we can proceed as follows (see Fig. 4):

i. draw "line zero" as the continuation of the α/β interface through the particle,

ii. draw "line a" being parallel to "line zero" and touching particle γ within phase α,

iii. draw "line b", being parallel to "line zero" and touching particle γ within phase β,

iv. measure distance h_α between "line zero" and "line a",

v. measure distance h_β between "line zero" and "line b", and

vi. substitute these values and the obvious relationship: $2 \cdot R_\gamma = h_\alpha + h_\beta$ into Eq. 4 to find the contact angle as:

$$\cos \Theta_{\gamma/\beta/\alpha} = \frac{2 \cdot h_\beta}{h_\alpha + h_\beta} - 1 \tag{5}$$

The application of Eq. 5 is connected with the following practical problems:

i. If the contact angle is 0 or 180° (or around these values), the majority of the particles are not positioned at the interface, and thus quantities h_α and h_β are not measurable (see Fig. 2).

ii. If the position of the particle is significantly changed during cooling and solidification, Eq. 5 would provide wrong results. In this paper we suppose that the interfacial capillary forces keeping the particles at an equilibrium position at the interface [51] are much larger than the interfacial pushing force during solidification [51, 52], and thus the role of this effect is neglected here.

iii. If the particle is not exactly spherical, Eq. 5 is not exactly valid. However, if different diameters of a non-spherical particle measured along different direction through its centre of mass do not differ significantly, Eq. 5 can be applied as an approximation.

iv. Equation 5 is applicable only, if the cross section is made in the plane through the centre of a spherical particle and if it is perpendicular to the α/β interface. This condition is generally not satisfied. However, if a large number of particles are analyzed in different,

Table 4 Geometrical arrangements in the $\alpha/\beta/\gamma$ system as function of contact angle $\Theta_{\alpha/\beta/\gamma}$

Contact angle (°)	Form of droplet β on solid γ under liquid α	Position of a single particle γ at the α/β interface	Distribution of γ particles between phases α and β
0	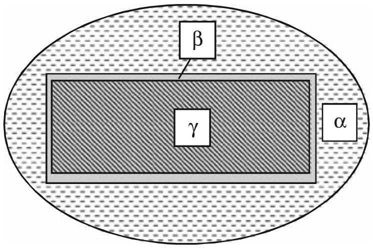	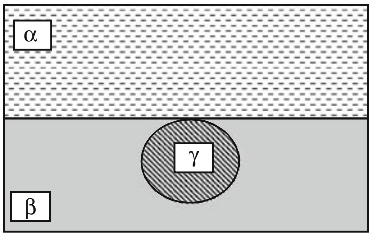	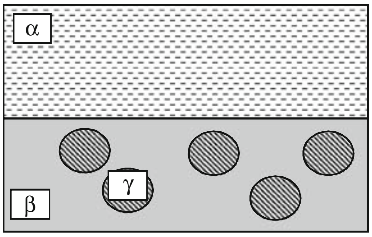
30	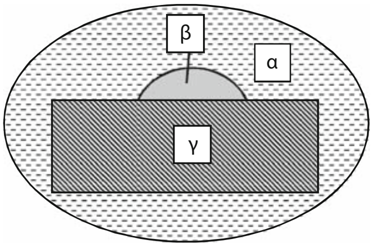	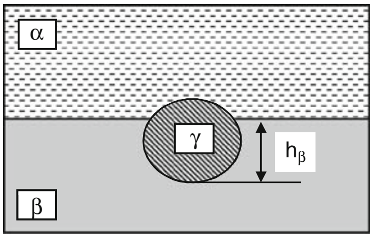	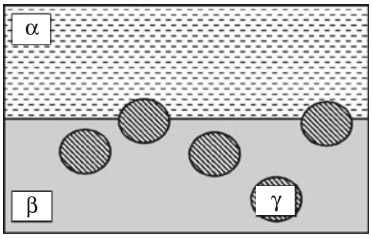
90	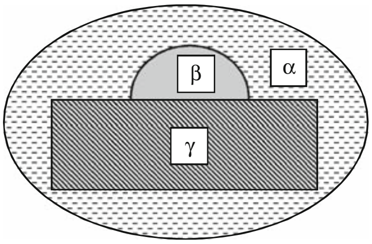	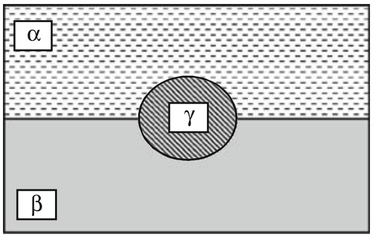	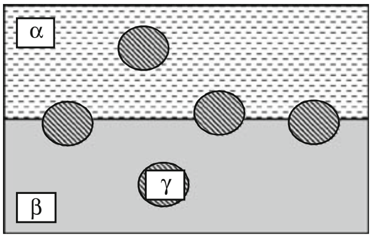
120	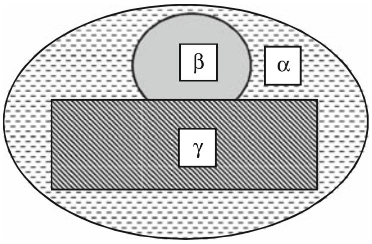	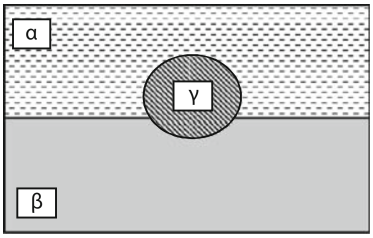	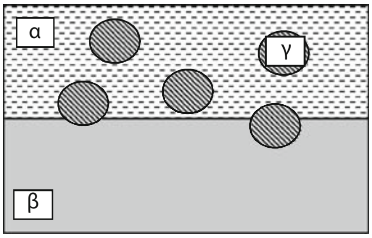
180	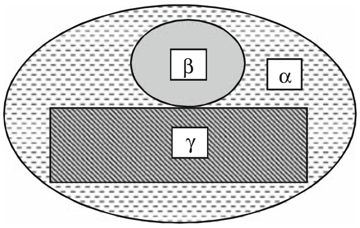	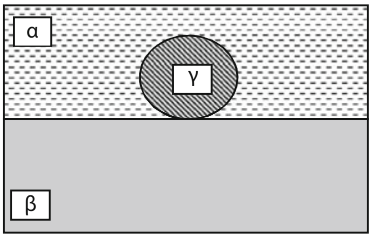	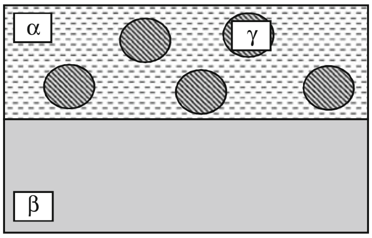

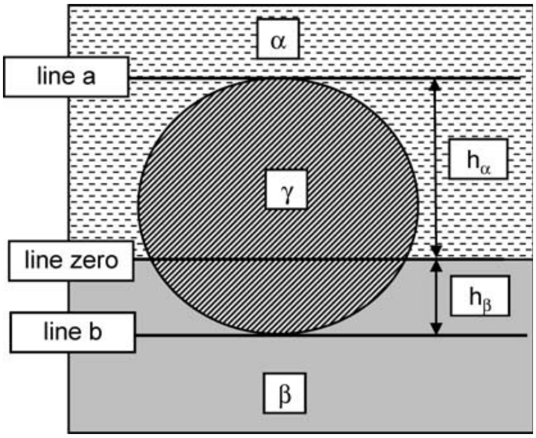

Fig. 4 Schematic construction to find h_β and h_α for Eq. 5. Particle γ is positioned at the interface of phases α and β. The continuation of the interface is called "line zero". The two parallel lines ("line a" and "line b") are drawn to touch the particle at one point within phases α and β. Using this method, the distances h_β and h_α are measured as shown. This information is substituted into Eq. 5 to calculate the contact angle

random planes, an average value of the contact angle calculated by Eq. 5 will provide a value being close to the real contact angle.

Thus, although statistically only, Eq. 5 can be applied to evaluate the contact angle in our systems. From Fig. 2 one can see that Eq. 5 is not applicable for sample 1, as all the alumina particles are positioned within the Bi-rich phase and thus h_α and h_β are not measurable.

As follows from Fig. 3, Eq. 5 is applicable to sample 2, as most of the particles are positioned along the interface. Applying the above method to 100 SiC particles in Fig. 3 and in similar figures (not shown here), the average contact angle was found to be: $\Theta_{\gamma/\beta/\alpha} = 81° \pm 18°$.

The method based on the distribution of particles

Let us again suppose that we have good quality micrographs of the cross section of solidified samples, showing many solid particles γ distributed among phases α and β. Let us suppose that the majority of particles are not situated along the α/β interface, or the position of a single particle is hard to determine in details. In this case the contact angle will be evaluated from the distribution of particles (see Table 4). A given solid particle γ can be situated in the following three positions in the α/β system:

i. the particle can be entirely within phase α (called "position α" hereinafter),
ii. the particle can be entirely within phase β (called "position β" hereinafter), and
iii. the particle can be at the α/β interface, i.e. the α/β interface intersects the particle (called "position i" hereinafter (i = interface)).

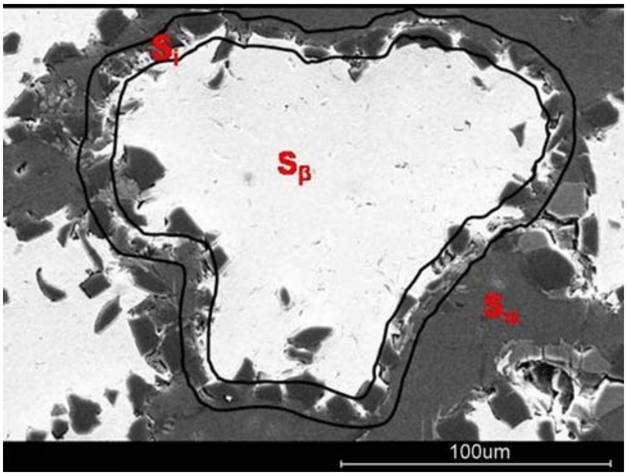

Fig. 5 Surface areas covered by phases α and β and by the interfacial phase i (see Fig. 3)

From the micrograph the number of particles in the three positions can be found, to be denoted as N_α, N_β and N_i, respectively. Also, the surface areas covered by different phases can be found as shown in Fig. 5. For this, two lines should be drawn parallel to each α/β interface with a distance of R_γ (the average radius of the particle) from the original α/β interface towards both phases α and β. The area between these two parallel lines (with their distance of $2R_\gamma$) is the area of the interface, S_i (see Fig. 5). Then, the surface area weighed number fractions of particles can be obtained in the three positions as follows:

$$x_\alpha = \frac{\frac{N_\alpha}{S_\alpha}}{\frac{N_\alpha}{S_\alpha} + \frac{N_\beta}{S_\beta} + \frac{N_i}{S_i}} \tag{6a}$$

$$x_\beta = \frac{\frac{N_\beta}{S_\beta}}{\frac{N_\alpha}{S_\alpha} + \frac{N_\beta}{S_\beta} + \frac{N_i}{S_i}} \tag{6b}$$

$$x_i = 1 - x_\alpha - x_\beta \tag{6c}$$

From Table 4 the following boundary conditions can be found:

i. If $x_\alpha = 1$, i.e. when all particles γ are within phase α, then $\Theta_{\gamma/\beta/\alpha} = 180°$.
ii. If $x_\beta = 1$, i.e. when all particles γ are within phase β, then $\Theta_{\gamma/\beta/\alpha} = 0°$.
iii. If $x_i = 1$, i.e. when all particles γ are at the α/β interface, then $\Theta_{\gamma/\beta/\alpha} = 90°$.
iv. If $x_\alpha = x_\beta$, i.e. when the probabilities that particles γ are within phase α and phase β equal, then obviously $\Theta_{\gamma/\beta/\alpha} = 90°$.

Now, let us suppose that the cosine of the contact angle is a linear combination of x_α. Then, using the first two boundary conditions, the following approximated equation is obtained:

$$\cos\Theta_{\gamma/\beta/\alpha} \cong x_\beta - x_\alpha \tag{6d}$$

One can see that Eq. 6d automatically satisfies also the above 3rd and 4th boundary conditions. That is why, we accept Eq. 6d in the first approximation. Substituting Eqs. 6a–c into Eq. 6d, the following final equation is obtained:

$$\cos\Theta_{\gamma/\beta/\alpha} \cong \frac{\frac{N_\beta}{S_\beta} - \frac{N_\alpha}{S_\alpha}}{\frac{N_\alpha}{S_\alpha} + \frac{N_\beta}{S_\beta} + \frac{N_\mathrm{i}}{S_\mathrm{i}}} \tag{6e}$$

The application of Eq. 6e is connected with similar practical problems as that of Eq. 5. Nevertheless, let us suppose that if a large number of particles in each micrograph and a large number of micrographs are taken into account, Eq. 6e provides statistically reasonable values.

As one can see from Fig. 2, all alumina particles are fully embedded in the Bi-rich liquid phase. None of the particles are situated at the interface or within the Al-rich phase. Thus, Eq. 5 is not applicable for this case and only Eqs. 6d–e can be used to calculate the contact angle. From Fig. 2 it becomes obvious that $x_\beta = 1, x_\alpha = 0$ in this case. The same result follows from other micrographs not shown here. Substituting this result into Eq. 6d, the contact angle follows as: $\Theta_{\gamma/\beta/\alpha} = 0°$. The same result follows also from Table 4.

As one can see from Fig. 3, the SiC particles are more or less evenly distributed between the Al-rich and the Bi-rich phases, while the majority of the SiC particles are positioned along the interface. From Figs. 3 and 5, the following primary results are obtained: $N_\alpha = 3$, $N_\beta = 15$, $N_\mathrm{i} = 48$, $S_\alpha = 31.0$ a.u., $S_\beta = 50.7$ a.u., $S_\mathrm{i} = 18.3$ a.u. Substituting these values into Eq. 6e, the final result is obtained as: $\Theta_{\gamma/\beta/\alpha} = 86.2°$. Repeating the same procedure for 10 micrographs and two samples (i.e. total 20 micrographs), the average contact angle for sample 2 is found as: $\Theta_{\gamma/\beta/\alpha} = 88° \pm 4°$. This result is in good agreement with the result obtained in the above sub-section ($\Theta_{\gamma/\beta/\alpha} = 81° \pm 18°$). One can see that Eq. 6e provides a smaller scatter compared to Eq. 5. This is due to the fact that in Eq. 5 each particle provides one value of the contact angle, while in Eq. 6e already a large number of particles are taken into account in each micrograph. That is why, the value of $\Theta_{\gamma/\beta/\alpha} = 88° \pm 4°$ is accepted in this paper.

Discussion

The experimental results found in this paper are summarized in Table 5. The result found for sample 1 is in perfect agreement with that obtained previously by Hoyer et al. [15] (see Table 1). This agreement validates our new method of measurement of contact angles in immiscible liquid alloys. Unfortunately, we have found no data in the literature that could be compared to our sample 2. That is why the contact angle found for sample 2 is considered here as a new experimental result. The authors are looking forward to see experimental results for the same system to be obtained by independent methods.

Table 5 Summary of the experimental results at 700 °C found in this paper

Sample	α phase	β phase	γ phase	$\Theta_{\gamma/\beta/\alpha}$ (°)
1	$Al_{98.8}Bi_{1.2}$	$Bi_{96.6}Al_{3.4}$	Al_2O_3	0
2	$Al_{91.2}Si_{7.2}Bi_{1.3}Mg_{0.3}$	$Bi_{94.7}Al_{3.8}Mg_{1.1}Si_{0.4}$	SiC	88 ± 4

Our experimental data can be used to evaluate the potential of different materials combinations to produce particles stabilized liquid metallic emulsions. In our previous theoretical paper on stabilization of emulsions by solid particles, the following intervals of contact angles were found [23]:

i. If the contact angle is below 15° or above 165°, particles are not able to stabilize liquid emulsions. This is the case for our sample 1 (the Al_2O_3/Bi/Al system), with the contact angle of 0°. Indeed, as was experimentally proven in our recent paper [16], stable emulsions in this system are not formed.
ii. If the contact angle is between 15 and 165°, the stabilization of emulsions by solid particles becomes possible. Particularly, if the contact angle is around 90° (in the interval between 70 and 110°), both types of emulsions (Bi droplets in Al-matrix or Al droplets in Bi-matrix) can form, depending on the volume fraction of the two liquid phases. This is the case for our sample 2 (the SiC/Bi/Al system), with contact angle around 88°. The formation of stable emulsions was proven experimentally in our previous paper [16].

Conclusions

The contact angles of liquid metals on solid substrates under an immiscible liquid metal have been defined. It is shown that these contact angles cannot be estimated from the existing databank on contact angle of liquid metals on the same solid substrates in gas environment. In this paper, one experimental and two approximated calculation methods have been developed to evaluate the contact angle in immiscible systems. The method has been validated for the alumina/Bi/Al system with zero contact angle measured, being in agreement with recent measured values using a different technique. The new value of the contact angle of about 88° has been measured in this paper for the SiC/Bi/A356 system. This contact angle value is ideal to produce SiC particles stabilized Al/Bi emulsions and monotectic alloys.

It should be underlined that both calculation methods presented in this paper are approximated. Their validity can be checked if the contact angle in the same system will be measured by the method described here and by independent methods in as many as possible systems. The authors hope that this will be done in the future and as a consequence, our approximated equations will be improved. However, in this paper the agreement found in one system out of the two measured systems is treated as a preliminary confirmation of our method.

Acknowledgements This work was partly financed by the NAP-NANO project (NKTH, Hungary) and partly by the Ministry of Education of Hungary as a PhD program for IB at the University of Miskolc, Hungary. The authors are grateful to A. Sytcheva for her help in SEM measurements. The authors are also grateful to L. Ratke, I. Kaban and R. Schmid-Fetzer for their discussions and encouragements.

References

1. Naidich JV (1981) Progr Surf Membr Sci 14:353
2. Eustathopoulos N, Nicholas MG, Drevet B (1999) Wettability at high temperatures. Pergamon, London
3. Kanai H, Sugihara S, Yamaguchi H, Uchimaru T, Obata N, Kikuchi T, Kimura F, Ichinokura M (2007) J Mater Sci 42:9529. doi:10.1007/s10853-007-2090-z
4. Li R, Ashgriz N, Chandra S, Andrews JR (2007) J Mater Sci 42:9511. doi:10.1007/s10853-007-1757-9
5. Gauffier A, Saiz E, Tomsia AP, Hou PY (2007) J Mater Sci 42:9524. doi:10.1007/s10853-007-2093-9
6. Aizenshtein M, Barzilai S, Froumin N, Frage N (2008) J Mater Sci 43:1259. doi:10.1007/s10853-007-2240-3
7. Protsenko P, Kozlova O, Voytovych R, Eustathopoulos N (2008) J Mater Sci 43:5669. doi:10.1007/s10853-008-2814-8
8. Boucherd D, Leboeuf S, Nadeau JP, Guthrie RIL, Isac M (2009) J Mater Sci 44:1923. doi:10.1007/s10853-008-2888-3
9. Lopez VH, Kennedy AR (2006) J Colloid Interface Sci 298:356
10. Good RJ, Givens WG, Tucek CS (1963) Adv Chem Series 43:211
11. Chatain D, Martin-Garin L, Eustathopoulos N (1982) J Chim Phys 79:569
12. Merkwitz M, Weise J, Thriemer K, Hoyer W (1998) Z Metallkd 89:247
13. Rivollet I, Chatain D, Eustathopoulos N (1990) J Mater Sci 25:3179. doi:10.1007/BF00587671
14. Merkwitz M, Hoyer W (1999) Z Metallkd 90:363
15. Hoyer W, Kaban I, Merkwitz M (2008) Phase transformations in multicomponent melts. Wiley-VCH, Weinheim, chap 2, pp 19–38
16. Budai I, Kaptay G (2009) Metall Mater Trans A 40A:1524
17. Zhao JZ, Ratke L (2004) Scr Mater 50:543
18. Wang CP, Liu XJ, Ohnuma I, Kainuma R, Ishida K (2002) Science 297:990
19. Wu M, Ludwig A, Ratke L (2003) Metall Mater Trans 34A:3009
20. Gao L, Zhao J, He J (2006) Spec Casting/Nonferr Alloys 26:626
21. He J, Zhao J, Wang X, Zhang Q, Li H, Chen G (2007) Acta Met Sin 43:561
22. Binks BP (2002) Curr Opin Colloid Interface Sci 7:21
23. Kaptay G (2006) Coll Surf A 282–283:387
24. Mott BW (1968) J Mater Sci 3:424. doi:10.1007/BF00550987
25. Singh RN, Sommer F (1997) Rep Prop Phys 60:57
26. Gröbner J, Schmid -Fetzer R (2005) JOM 1:9
27. Curiotto S, Battezzati L, Johnson E, Palumbo M, Pryds N (2008) J Mater Sci 43:3253. doi:10.1007/s10853-008-2540-2
28. Nag S, Mahdak KC, Devaraj A, Gohil S, Ayyub P, Banerjee R (2009) J Mater Sci 44:3393. doi:10.1007/s10853-009-3449-0
29. Zhou ZM, Gao J, Li F, Zhang YK, Wang YP, Kolbe M (2009) J Mater Sci 44:3793. doi:10.1007/s10853-009-3511-y
30. Mirkovic D, Gröbner J, Kaban I, Hoyer W, Schmid-Fetzer R (2009) Int J Mater Res 100:176
31. Kaban J, Gröbner W, Hoyer W, Schmid-Fetzer R (2009) J Mater Sci (this issue)
32. Young T (1805) Philos Trans 65
33. Kaptay G (2005) Mater Sci Forum 473–474:1
34. Kaptay G (2008) Calphad 32:338
35. Keene BJ (1993) Int Mater Rev 38:157
36. Hoyer W, Kaban I, Merkwitz M (2003) J Optoelectr Adv Mater 5:1069
37. Kaban I, Hoyer W, Merkwitz M (2003) Z Metallkd 94:831
38. Champion JA, Keene BJ, Sillwood JM (1969) J Mater Sci 4:39. doi:10.1007/BF00555046
39. Laurent V, Chatain D, Chatillon C, Eustathopoulos N (1988) Acta Metall 36:1797
40. Kaptay G, Báder E, Bolyán L (2000) Mater Sci Forum 329–330:151
41. Sobczak N, Asthana R, Ksiazek M, Radziwill W, Mikulowski B (2004) Metal Mater Trans 35A:911
42. Shen P, Fujii H, Matsumoto T, Nogi K (2005) J Mater Sci 40:2329. doi:10.1007/s10853-005-1954-3
43. Menon VB, Wasan DT (1986) Colloid Surf 19:89
44. Hadjiiski A, Dimova R, Denkov ND, Ivanov IB, Borwankar R (1996) Langmuir 12:6665
45. Hórvölgyi Z, Máté M, Dániel A, Szalma J (1999) Colloid Surf A 156:501
46. Tolnai G, Csempesz F, Kabai-Faix M, Kálmán E, Keresztes Z, Kovács AL, Ramsden JJ, Hórvölgyi Z (2001) Langmuir 17:2683
47. Fournier CO, Fradette L, Tanguy PA (2009) Chem Eng Res Des 87:499
48. Kaptay G (1996) Mater Sci Forum 215–216:459
49. Verezub O, Kaptay G, Matsushita T, Mukai K (2005) Mater Sci Forum 473–474:429
50. Kaptay G (1991) Mater Sci Forum 77:315
51. Kaptay G (2005) J Mater Sci 40:2125. doi:10.1007/s10853-005-1902-2
52. Kaptay G (2001) Metall Mater Trans A 32A:993